Joint time-lapse full-waveform inversion with a time-lag cost function

Zhiguang Xue, Zhigang Zhang, Ping Wang (CGG), and Jun Cai (BHP)*

Summary

Seismic time-lapse (4D) surveys have been widely used to quantitatively monitor the geophysical property changes within hydrocarbon reservoirs due to production effects. Full-waveform inversion (FWI), which has become one of the most reliable tools for velocity model building (VMB), is a natural technology choice for this purpose. However, robust reconstruction of time-lapse geophysical property changes within reservoirs using FWI remains challenging. Time-lapse signals are weak compared to the seismic response of the background model and thus vulnerable to noise and possible damage by data preprocessing. Imperfect repeatability of the baseline and monitor surveys also introduces uncertainties into the inverted time-lapse changes. To address these issues, we propose a 4D FWI approach, which jointly inverts both baseline and monitor data sets using a time-lag cost function with a target-oriented regularization scheme. This approach enhances the 4D signal within reservoirs while suppressing 4D noise away from them. We demonstrate our method using a synthetic and a field data example. We observe that it not only gives an interpretable 4D velocity difference, but also improves the 4D migration difference when compared with conventional 4D approaches.

Introduction

Time-lapse processing attempts to extract information of the geophysical property changes within reservoirs. Contrast of amplitude versus offset/angle (AVO/AVA) between the images from baseline and monitor data sets indicates variation of P- and S-wave velocity and density, which is related to pressure and fluid saturation changes (Landrø, 2001). As a common practice, the same velocity model is usually used for migrations of both baseline and monitor data, assuming the impact of 4D velocity changes to the migration difference is a second-order effect.

With improved algorithms and compute power, FWI has emerged as a routine tool for VMB and offers an alternative approach for directly characterizing time-lapse model changes within reservoirs. Straightforward subtraction of two separate FWI models using baseline and monitor data sets, or parallel inversion, has been applied to obtain the time-lapse changes within reservoirs (Kamei and Lumley, 2017). However, the results usually suffer from weak time-lapse signal of the 4D data and uncancelled inversion artifacts caused by the non-repeatability of the baseline and monitor acquisitions. Moreover, without a good starting model, the two inversion results may converge to different local minima (Mulder and Plessix, 2008). Various efforts have been carried out to tackle these issues. Double-difference inversion jointly inverts both baseline and monitor data sets, emphasizing the differences of time-lapse data during inversion. Therefore, double-difference inversion reduces the possibility of converging to different local minima for different data sets (Denli and Huang, 2009). However, double-difference inversion requires nearly perfect repeatability of the time-lapse data, which becomes an obstacle for field data applications. The sequential approach inverts the baseline and monitor data sets in the order of recording time. Its application requires neither perfect repeatability nor an accurate starting model (Asnaashari et al., 2014). Nonetheless, a better starting model and data repeatability are preferred for optimal inversion results. Target-oriented inversion aims to reduce the model space of the inversion to the area of interest, which is valid for 4D applications, but it usually assumes good accuracy in the area outside of the target, which is not always applicable (Malcolm and Willemsen, 2016).

We propose an FWI approach that jointly inverts baseline and monitor data sets to reconstruct both baseline and monitor models at the same time. This approach does not require perfect repeatability of the two acquisitions. The combined data sets include more input seismic traces, which increases constraints on the output models. In addition, we apply a time-lag cost function to leverage the stable performance of Time-lag FWI (TLFWI) for different data types and different geologic settings (Zhang et al., 2018; Wang et al., 2019). Furthermore, a target-oriented regularization approach is used to enhance 4D signals in the reservoirs as well as to suppress 4D noise caused by poor data repeatability and possible crosstalk between the inverted baseline and monitor models away from the reservoirs. The synthetic and field data examples demonstrate the effectiveness of our approach in building the time-lapse model and reducing the 4D noise when the respective 4D FWI models are used to migrate the baseline and monitor data.

Method

FWI inverts the subsurface model by minimizing the difference between synthetic and recorded seismic data (Lailly, 1983; Tarantola, 1984). Alternatively, TLFWI adapts the inversion with a kinematics-only cost function to mitigate the cycle-skipping and amplitude-discrepancy issues as follows (Zhang et al., 2018):

$$\chi(v) = \sum_{s,r,w} c\Delta\tau^2, \tag{1}$$

where v is the velocity model, c is a crosscorrelation coefficient between the recorded data and modeled synthetic data, w is the window index, $\Delta\tau$ is the time shift between the recorded data and modeled synthetic data, and s and r are the source and receiver index, respectively.

For time-lapse data, we propose to invert the baseline and monitor data sets jointly:

$$\chi(v_b, v_m) = \sum_{s_b,r_b,w_b} c_b\Delta\tau_b^2 + \sum_{s_m,r_m,w_m} c_m\Delta\tau_m^2 + \lambda_1\left|\left|S(v_m - v_b)\right|\right|_{TV} + \lambda_2\left|\left|(1-S)(v_m - v_b)\right|\right|_2^2, \tag{2}$$

where the subscripts b and m refer to baseline and monitor. The TV-norm is defined as

$$\left|\left|v\right|\right|_{TV} = \sum_i \sqrt{|\nabla_x v_i|^2 + \left|\nabla_y v_i\right|^2 + |\nabla_z v_i|^2}, \tag{3}$$

where i is the index of spatial grids in a Cartesian coordinate (x, y, z). The scaling factor $S \in [0, 1]$ is designed based on a target interpretation with a value of 1 in the reservoir and a value of 0 far away from it. The third and fourth terms in Equation 2 effectively apply a TV regularization for suppressing 4D noise while preserving 4D structures when $S = 1$, a Tikhonov regularization for tying baseline and monitor models when $S = 0$, and a linear combination of them when $S \in (0,1)$. The regularization parameters λ_1 and λ_2 are defined into physically meaningful scales based on the initial velocity model, and, in practice, the optimal parameters fall into a relatively narrow range of values. This approach does not require perfect repeatability of the two surveys, as baseline and monitor data are exclusively in the first and second terms.

Synthetic and field data examples

Figure 1a shows the 2D model for our synthetic tests. A towed-streamer acquisition survey was generated, consisting of 800 shots spaced every 25 m. Each shot contained 800 receivers. We generated the synthetic data using a Ricker wavelet centered at 25 Hz. We started our FWI tests from a smoothed version of the baseline model (Figure 1b). The monitor model differed from the baseline model in one target area (Figure 1c). The difference of the migration images using baseline and monitor data based on true models serves as a reference for the later test results (Figure 1d).

For this synthetic example, we compared different 4D FWI approaches using the same time-lag misfit function but with different inversion strategies: parallel, double-difference, and joint inversion. The time-lapse velocity result of parallel inversion is shown in Figure 2a. Although the velocity within the target area is well inverted, parallel inversion leaves strong perturbation leakage in the background model. As a result, the 4D migration difference (Figures 2b) exhibits noise beneath the target area. Compared to the parallel approach, the double-difference method results in reduced leakage in the velocity model given this perfectly repeated synthetic data (Figure 2c), but with a similar 4D migration difference (Figure 2d). Our proposed method updates both the baseline and monitor models in one joint inversion. It leads to a much more focused 4D velocity difference (Figure 2e) and reduced 4D migration noise (Figure 2f) than the double-difference approach. Among all three 4D FWI approaches, joint 4D FWI gives 4D velocity and migration differences that best resemble the reference results in Figures 1c and 1d for this synthetic example.

The field data example is from the Pyrenees field off the coast of Exmouth, Western Australia. The baseline and monitor data sets were acquired in 2006 and 2013, respectively. Both surveys have a cable length of 3600 m, but with different cable depths: 6 m for the baseline data set and 15 m for the monitor data set. The reservoir is situated at a depth of 1200 m, which is around the limit of the diving wave penetration depth of these acquisitions.

The conventional 4D approach, where the 4D migration difference from the baseline and monitor data sets is obtained using a common velocity model (the one obtained by 3D FWI using both baseline and monitor data), shows clear 4D signal at the reservoir level and some spurious 4D differences (red arrow) in the deeper area (Figures 3a and 3d). Figures 3b and 3c show the baseline and monitor models from joint 4D FWI, respectively. The direct subtraction of both models gives clear 4D velocity signal around the reservoir (Figure 3e). The new 4D migration difference from the baseline and monitor data sets using their corresponding velocity models from joint 4D FWI is shown in Figure 3f, with no sign of the spurious 4D difference we see in Figure 1d. This indicates that the 4D velocity difference in the reservoir is significant and, thus, cannot be ignored for the 4D migration difference. Figure 4 compares the surface offset gathers below the reservoir of the monitor data migrated using the common velocity model (Figure 4a), i.e., the velocity model used for conventional 4D migration, and the monitor model from joint 4D FWI (Figure 4b). Our joint 4D monitor model gives better event focusing and flatter gathers (box in Figure 4b).

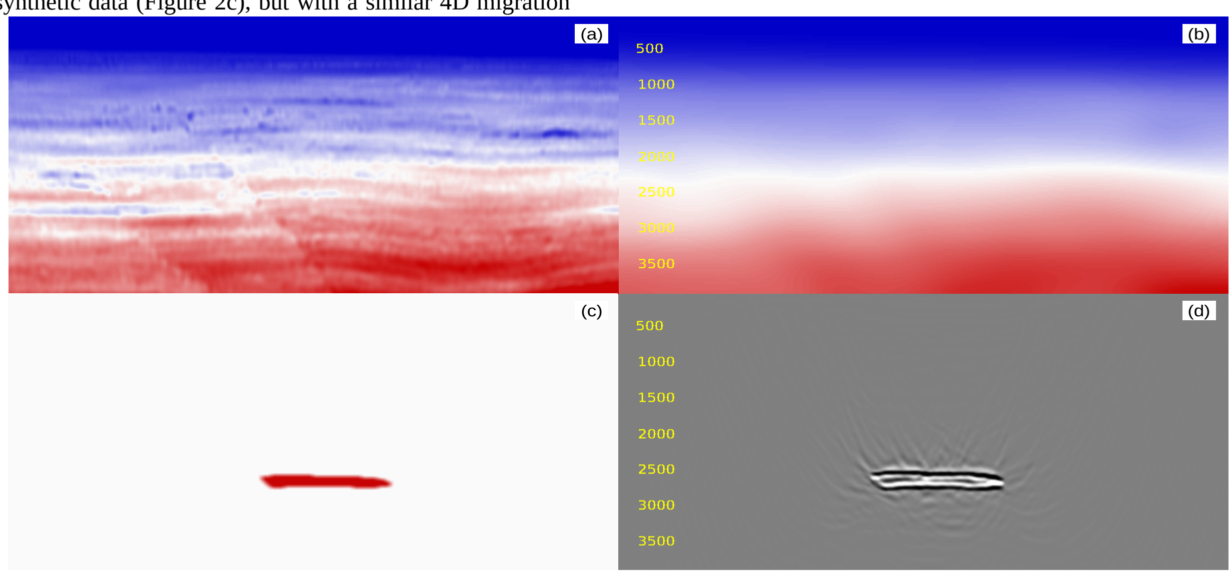

Figure 1. (a) The true baseline model, (b) the initial model for FWI tests, (c) the true time-lapse difference in the target, and (d) the 4D migration difference using the true baseline and monitor models.

10.1190/segam2021-3594752.1

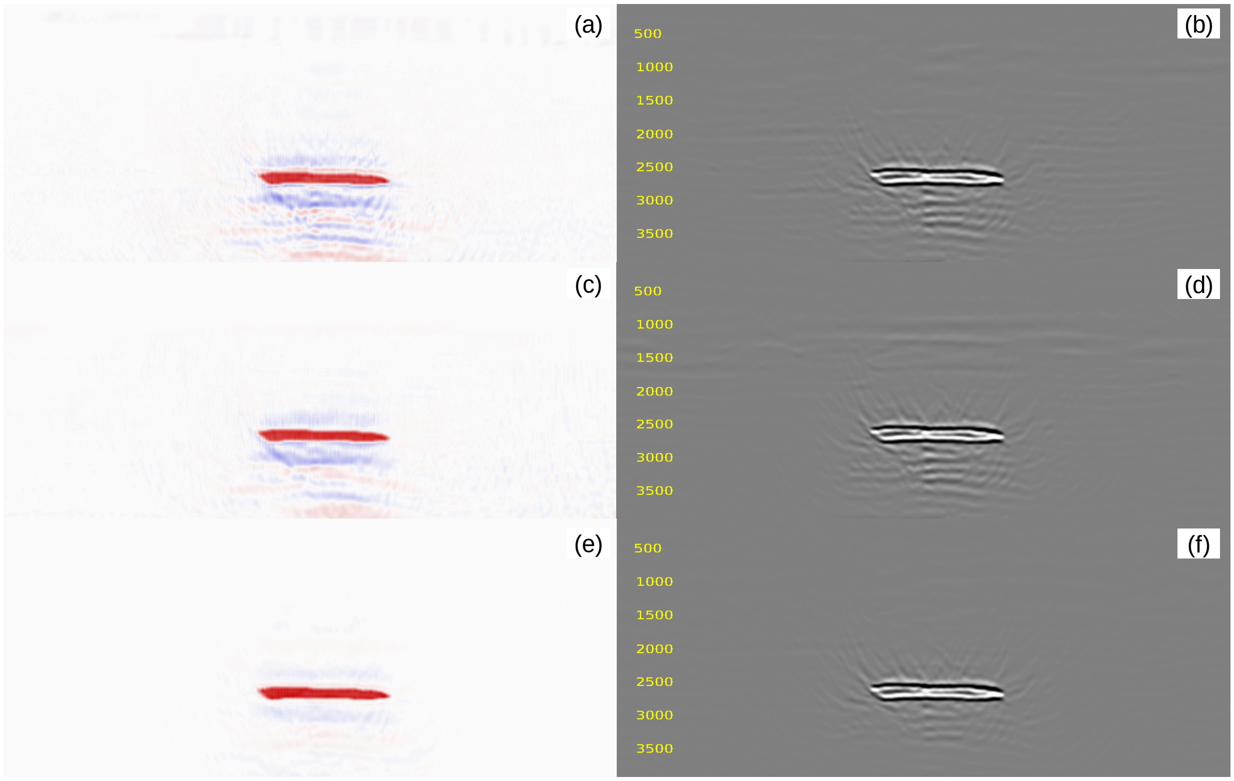

Figure 2. (a) 4D velocity difference by parallel inversion and (b) corresponding 4D migration difference; (c) 4D velocity difference by double-difference inversion and (d) corresponding 4D migration difference; (e) 4D velocity difference by joint 4D FWI and (f) corresponding 4D migration difference.

Conclusions and discussion

We implemented a joint 4D FWI scheme that simultaneously inverts for the baseline and monitor models using a time-lag cost function and a target-oriented regularization term. The time-lag cost function can better tackle the common issues of FWI, such as cycle-skipping and amplitude-mismatching between modeled data and recorded data. The target-oriented regularization scheme can enhance the 4D signals in the reservoirs while suppressing 4D noise away from them. Using both synthetic and field data examples, we demonstrated that it provides directly interpretable 4D velocity signals that are consistent with 4D migration signals and production history. It also reduces 4D migration noise by providing respective velocity models to migrate the baseline and monitor data correspondingly. Compared to the common velocity model obtained by 3D FWI, the monitor model from joint 4D FWI gives better event focusing and gather flatness for the monitor data as well as reduced 4D noise below the reservoirs.

Conventionally, strenuous preprocessing steps with extra caution must be carried out to reduce 4D noise from different sources. However, it is very difficult to remove all noise perfectly without preprocessing-induced 4D noise and signal damage. FWI is resilient to noise in the input data because of its inherent stacking procedure. Our proposed joint 4D FWI approach can use input data sets with minimal preprocessing, which reduces the chance of signal damage and significantly reduces the turnaround time.

The 4D signal in the migration difference is usually much weaker than the 3D migration amplitude, and the 4D velocity difference is often even weaker. For this reason, 4D velocity signals can be easily overwhelmed in joint 4D FWI by imperfections such as initial model inaccuracy and input non-repeatability.

The quality of the initial model plays a crucial role in 4D FWI-based VMB. When the error in the initial model is substantial, separate inversions, either parallel or sequential, could converge to quite different local minima. On the other hand, our joint 4D FWI tries to explain both input data sets with a consistent/4D-friendly pair of baseline and monitor models. While this process effectively reduces the risk of converging into two very different local minima, the inversion could still fall into a common or similar local minimum that causes suboptimal 4D signals due to poor focusing and additional 4D noise due to migration artifacts. Therefore, joint 4D FWI needs to start from an initial model that is as good as possible since the 4D velocity difference is usually very small.

Repeatability is a vital component in conventional 4D processing. Although our joint 4D FWI approach theoretically does not require perfect repeatability of the input data, we note that good repeatability is still key to its success since the 4D velocity difference is usually very small. While evolving technology and acquisition design continue to improve the repeatability of time-lapse data, flawless repeatability has yet to become a reality. Therefore, 4D-binning, which is commonly used in conventional 4D processing, is still recommended to enhance the repeatability of the input data to joint 4D FWI. Furthermore, a carefully designed target-oriented regularization scheme has an important role in suppressing the 4D noise associated with residual non-repeatability.

Acknowledgments

We thank BHP and CGG for permission to publish this work. We are grateful to Zhuocheng Yang, Shouting Huang, Yuan Zhang, and Sabaresan Mothi for learnings from their investigation of the problem.

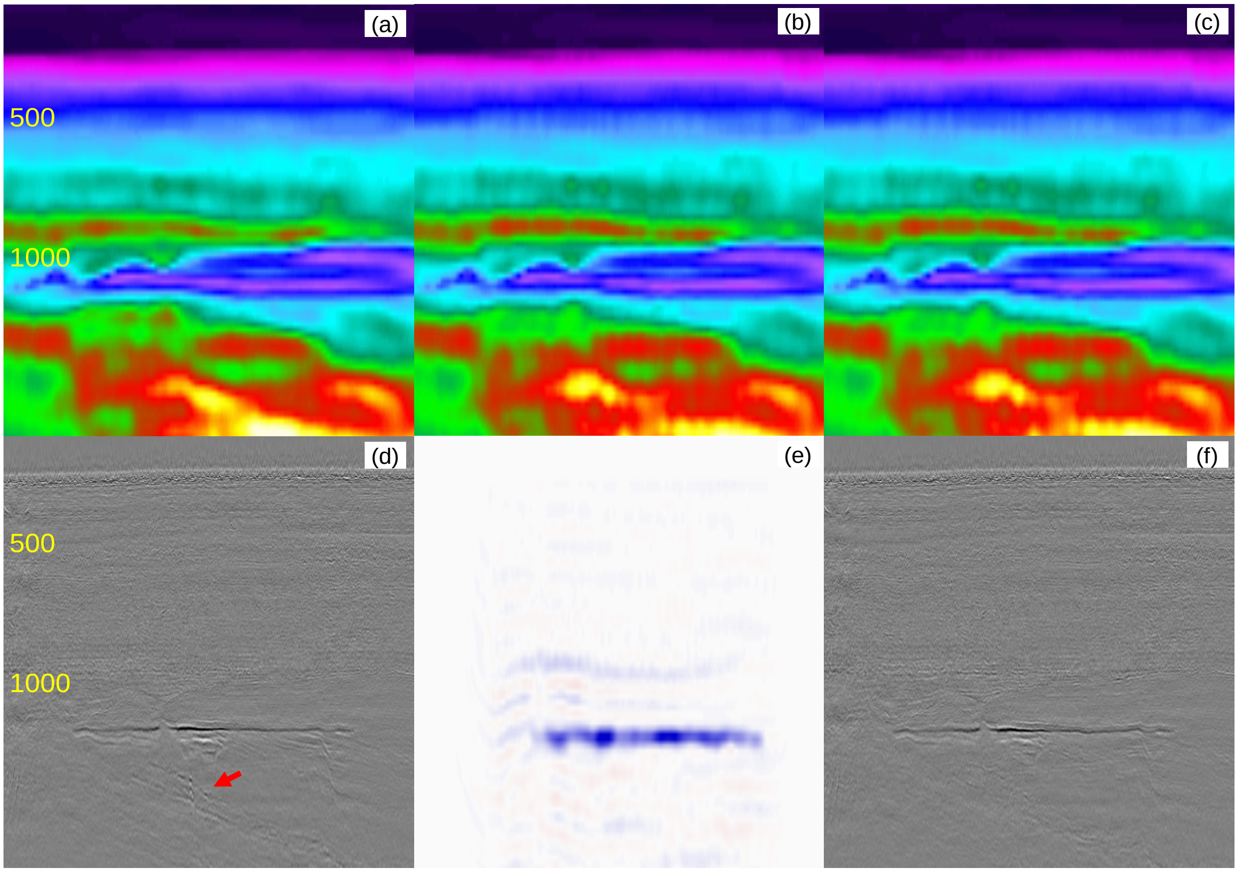

Figure 3. (a) The common velocity model inverted by 3D FWI using both baseline and monitor data sets and (d) 4D migration difference using the same model in (a). Inverted (b) baseline and (c) monitor models from joint 4D FWI; (e) the 4D model difference of (c-b), and (f) the 4D image difference using respective joint 4D FWI models (b/c) to migrate baseline/monitor data.

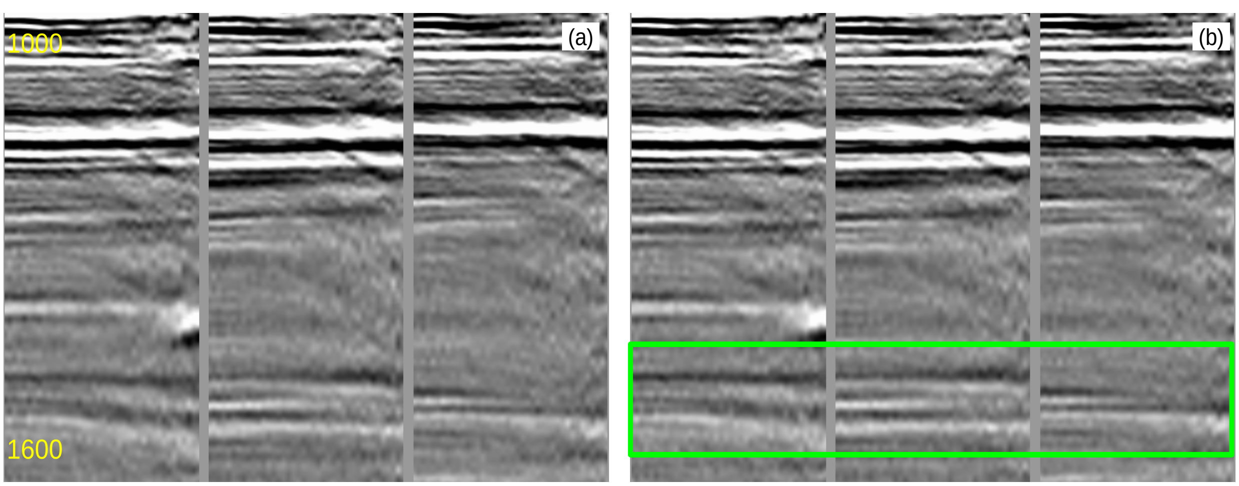

Figure 4. Gathers of monitor data beneath reservoir using (a) the common model from 3D FWI (Figure 3a) and (b) the monitor model from joint 4D FWI (Figure 3c).

REFERENCES

Asnaashari, A., R. J. Brossier, S. Garambois, F. Audebert, P. Thore, and J. Virieux, 2015, Time-lapse seismic imaging using regularized full-waveform inversion with a prior model: Which strategy?: Geophysical Prospecting, **63**, 78–98, doi: https://doi.org/10.1111/1365-2478.12176.

Denli, H., and L. Huang, 2009, Double-difference elastic waveform tomography in the time domain: 79th Annual International Meeting, SEG, Expanded Abstracts, 2302–2306, doi: https://doi.org/10.1190/1.3255320.

Kamei, R., and D. Lumley, 2017, Full waveform inversion of repeating seismic events to estimate time-lapse velocity changes: Geophysical Journal International, **209**, 1239–1264, doi: https://doi.org/10.1093/gji/ggx057.

Lailly, P., 1983, The seismic inverse problem as a sequence of before stack migrations: Conference on Inverse Scattering: Theory and Application, SIAM, 206–220.

Landrø, M., 2001, Discrimination between pressure and fluid saturation changes from time-lapse seismic data: Geophysics, **66**, no. 3, 836–844, doi: https://doi.org/10.1190/1.1444973.

Malcolm, A., and B. Willemsen, 2016, Rapid 4D FWI using a local wave solver: The Leading Edge, **35**, 1053–1059, doi: https://doi.org/10.1190/tle35121053.1.

Mulder, W. A., and R. E. Plessix, 2008, Exploring some issues in acoustic full waveform inversion: Geophysical Prospecting, **56**, 827–841, doi: https://doi.org/10.1111/j.1365-2478.2008.00708.x.

Tarantola, A., 1984, Inversion of seismic reflection data in the acoustic approximation: Geophysics, **49**, no. 8, 1259–1266, doi: https://doi.org/10.1190/1.1441754.

Wang, P., Z. Zhang, J. Mei, F. Lin, and R. Huang, 2019, Full-waveform inversion for salt: A coming of age: The Leading Edge, **38**, 204–213, doi: https://doi.org/10.1190/tle38030204.1.

Zhang, Z., J. Mei, F. Lin, R. Huang, and P. Wang, 2018, Correcting for salt misinterpretation with full-waveform inversion: 88th Annual International Meeting, SEG, Expanded Abstracts, 1143–1147, doi: https://doi.org/10.1190/segam2018-2997711.1.

10.1190/segam2021-3594752.1